Crisis and intermittence in a leaky-faucet experiment

J. C. Sartorelli, W. M. Gonçalves and R. D. Pinto
Instituto de Física, Universidade de São Paulo, Caixa Postal 20516, 01452-990 São Paulo, Brazil
(Received 17 September 1993)

Two types of sudden changes in chaotic attractors were observed in a leaky-faucet experiment. One of them is consistent with a boundary crisis interpretation. Intermittent behaviors of two kinds were also observed. One type is related to a tangent bifurcation with odd periodic attractors and bursts of chaos, and the other type takes place between two even periodic attractors.

PACS number(s): 47.52.+j

I. INTRODUCTION

Chaotic behavior, periodic doubling, and intermittence related to tangent bifurcations in leaky-faucet experiments were observed by Martien *et al.* [1], Yépez *et al.* [2], Cahalan *et al.* [3], Wu and Schelly [4], and Dreyer *et al.* [5]. Some experimental data were simulated by Martien *et al.* [1], supposing that the forming drop in the faucet hole oscillates according to the mass-spring model

$$\frac{d}{dt}\left(m\frac{dy}{dt}\right) = mg - ky - b\frac{dy}{dt}, \tag{1}$$

where y is the forming drop position. The behavior of the solutions depends on the spring constant k, the friction constant b , $m(t)$, and g. With a decreasing frequency, the drop mass increases until it reaches a critical point and breaks away imposing the initial conditions for the next drop.

Grebogi *et al.* [6] demonstrated that in an one-dimensional quadratic map,

$$x_{n+1} = C - x_n^2 = F(x_n, C) \tag{2}$$

the basin of the attraction for $\frac{1}{4} \leq C \leq 2$ is $|x| \leq x_*$, where x_* are the unstable points given by $x_* = -\frac{1}{2} + \left(\frac{-1}{4} + C\right)^{\frac{1}{2}}$. The destruction of the chaotic attractor and its basin as C increases through $C = 2$ coincides with the intersection of the chaotic band with the unstable fixed point. These authors defined crisis as "a collision between a chaotic attractor and a coexisting unstable fixed point or periodic orbit" and stated that the interior crisis is the cause of almost sudden changes in the size of chaotic attractors, and almost all sudden destructions and creations of chaotic attractors and their basins are due to the *boundary crisis.*

Manneville *et al.* [7] studying the Lorentz model in detail observed periodic motions with bursts of chaos when the value of the control parameter (r) is close to the value at which the motion becomes periodic (r_c). The intermittent behavior occurs *when the parabolic curve intersects, then tangents and loses contact with the first bissetrix* (see Figs. 11 and 12 of Ref. [7], and Fig. 15 of Ref. [3] for a one-dimensional map), and the mean time duration of the periodic motion τ is proportional to $(r - r_c)^{-1/2}$.

The large water reservoirs of our equipment and the

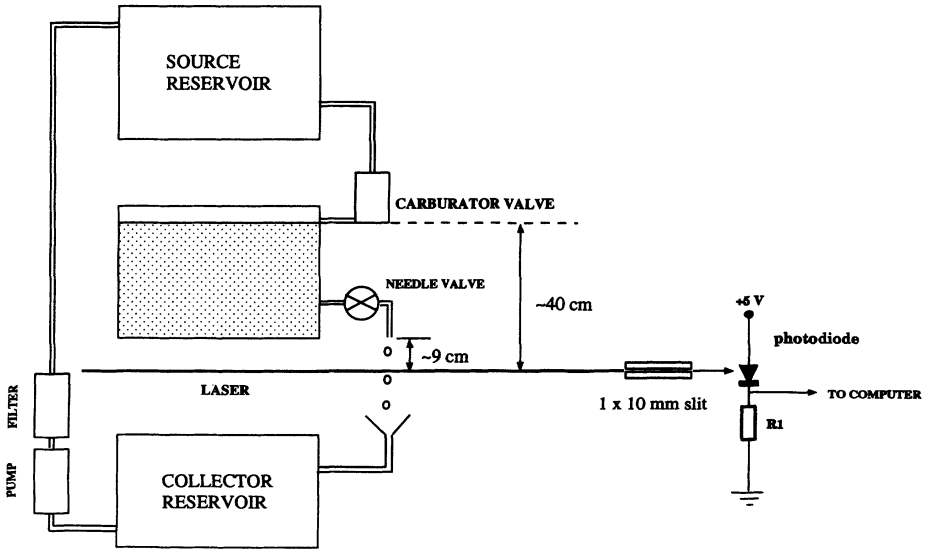

FIG. 1. Diagram of the experimental apparatus. The needle valve opening is controlled by a step motor driven by the computer.

care to take data during the weekends dawn hours only to avoid mechanical vibrations established a good stability to the water system and a precise flux control. The resolution of 10 μs of the driver program allowed us to construct two different kinds of return maps to typify the same motion. Therefore, we could observe the following.

(a) Two kinds of sudden changes of attractors or crisis, where we investigated transitions from chaotic to nonchaotic behaviors. In one case the transition is between chaotic and period-1 regimes, but with no appreciable change in the mean drop frequency. In another case the transition is between chaotic and period-5 behaviors with a drastic change in the mean drop frequency, from 25.8 drops/s in the chaotic regime to 38.3 drops/s in period-5 regime. This transition was also registered by a video camera. We related this kind of sudden changes in the attractors to a *boundary crisis type.*

(b) Tangent intermittence, related to odd periodic regime, was detected for low drop frequency (1.7 drops/s) as well as for 15.3 drops/s. We also observed a new type of intermittent behavior between even periodic attractors, around 1.3 drops/s and 1.65 drops/s, that follows the sequence

$$\text{period-2} \rightarrow \text{intermittence } 2 \Longleftrightarrow 4 \rightarrow \text{period-1}$$

for successive faucet openings.

II. EXPERIMENTAL APPARATUS

The experimental apparatus consists of three deionized water reservoirs of 50 liters each, as shown in Fig. 1. The top reservoir is the source reservoir for the middle one, which level is kept constant via a carburetor valve and the one at the bottom is the collector reservoir. The source and the middle reservoirs are coated with a thermal insulator material. The faucet is a needle valve whose opening is controlled by a step motor system, where each step corresponds to a needle rotation of 1/8 degree of arc.

The detection system consists of a He-Ne laser and a photodiode, as shown in Fig. 1. The induced pulse in the photodiode by the drop passage through the laser beam is detected via a microcomputer parallel port. When each drop starts (ends) to cross the laser beam a logic level change in the parallel port is detected, then a count variable c is reset and gated. The resolution of the driver program is 10 μs and the minimum detectable time interval is 45 μs, which allowed us to measure not only the time between drops but the crossing time of the drop through the laser beam.

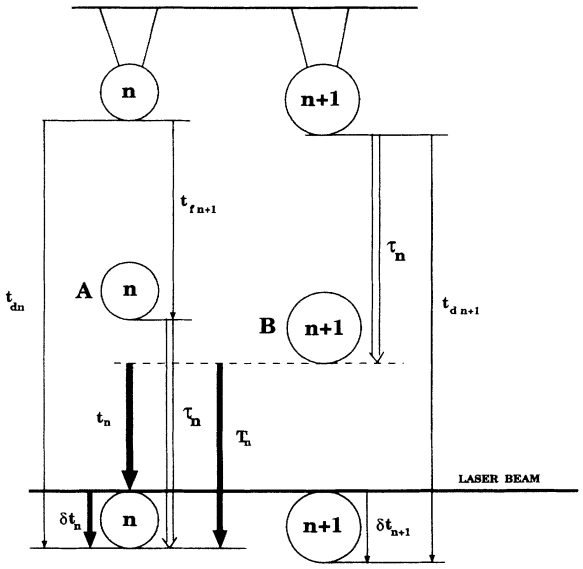

FIG. 2. Definition of the time intervals. The experimental time intervals (t_n, δt_n, and T_n) are shown in wide bold arrows.

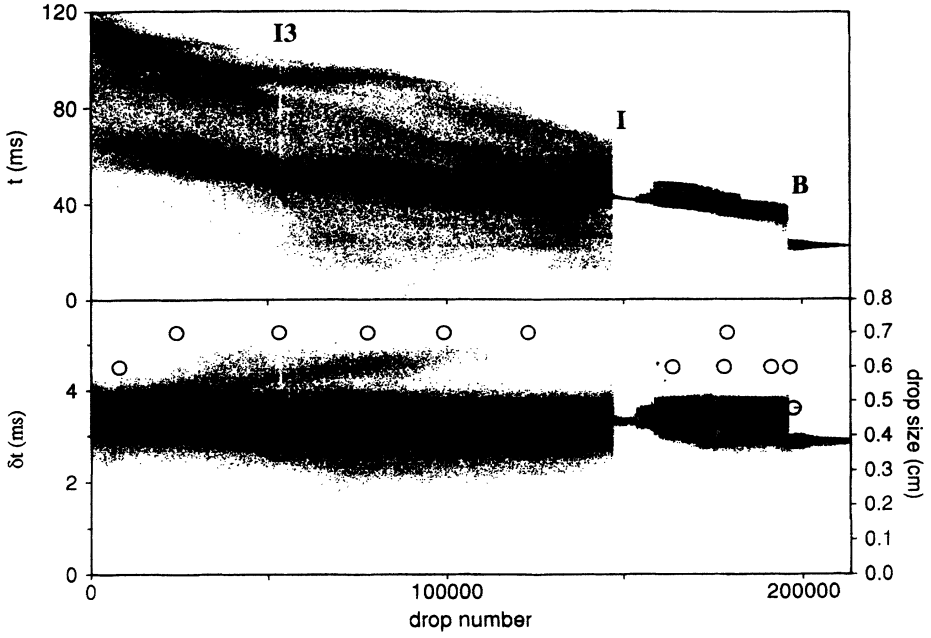

FIG. 3. An overview of a sequence of 208 sample data (each sample has 1024 data); t_n is the time between drops and δt_n is the crossing time through the laser beam. The discontinuity B is consistent with a boundary crisis interpretation. $I3$ is a periodic window. The circles are a crude estimation of the drop size.

In Fig. 2 we show a diagram to calculate the mean drop frequency. When the nth drop is ejected, the $(n+1)$th drop starts to grow and it will be formed after a time t_{fn+1}. At this time the nth drop will be at the A position. After a time τ_n the nth drop will be finishing to cross the laser beam and the $(n+1)$th drop will be reaching the B position. Therefore, introducing the definitions, t_d, as the time for a drop to go from the breakaway position until it finishes crossing the laser beam, δt, as the time for a drop to cross the laser beam, and t as the delay time between the back side of the nth drop and the front side of the $(n+1)$th drop, it is straightforward to show that

$$t_{fn+1} = t_n + \delta t_{n+1} + t_{dn} - t_{dn+1}. \tag{3}$$

The average time for the drop formation is given by

$$\langle t_f \rangle = \langle t \rangle + \langle \delta t \rangle = \langle T \rangle , \tag{4}$$

with the assumption that $\sum_n t_{dn} = \sum_n t_{dn+1}$, and $\sum_n \delta t_{n+1} = \sum_n \delta t_n$, so we define the mean drop frequency as $f = 1/\langle t_f \rangle$.

We have done two kinds of measurements (see wide bold arrows in Fig. 2): (a) the total time interval between successive drops (T_n); and (b) the time interval between drops (t_n) and the crossing time (δt_n) of the

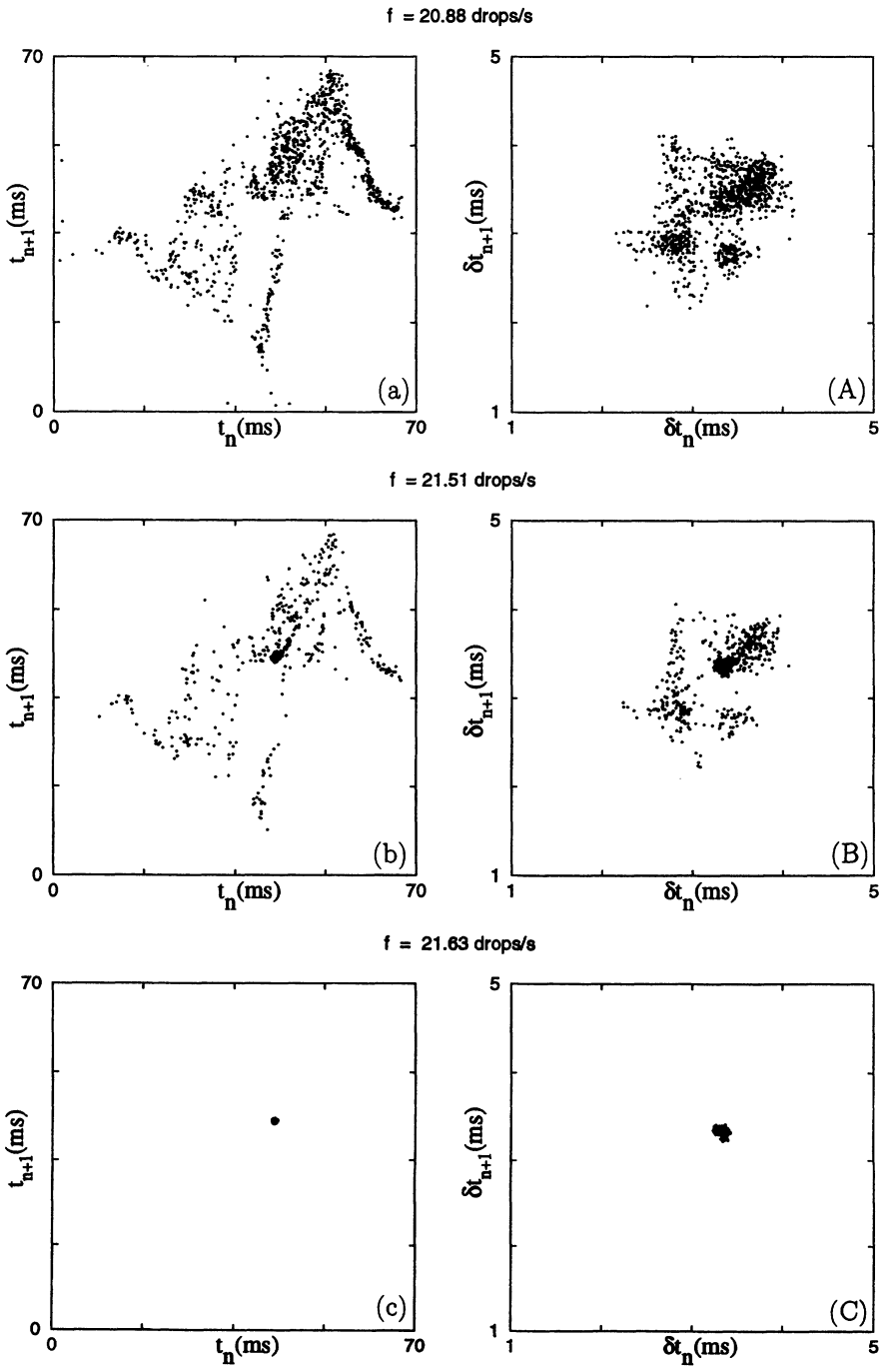

FIG. 4. Return maps of t_{n+1} vs t_n (left) and δt_{n+1} vs δt_n (right) of a sequence of three sample data. t_n is the time interval between drops and δt_n is the passage time of the drops through the laser beam. In (b) and (B) we show the transition from chaotic to period-1 behavior.

drop through the laser beam. In this case, t_n corresponds to the measurement of a coordinate of the nth drop relative to the $(n+1)$th drop, while δt_n is a measurement of an absolute coordinate of the nth drop. Therefore two kinds of return maps were constructed, t_{n+1} vs t_n and δt_{n+1} vs δt_n, to typify the same motion. Since the drop velocity at the laser beam level is $v_n = D_n/\delta t_n$, then the return map δt_{n+1} vs δt_n must be correlated in some way to the drop escape velocity.

The data were collected, in several runs, from a rate of 1 drop/s up to 40 drops/s, approximately (close to the point where the water flux becomes continuous). The water flux was increased by successively opening the faucet step by step. For each faucet opening, and after an awaiting time of 10–15 s for the stabilization of the system, a sample of data of 1024 drops was taken. We defined as a sequence a collection of samples obtained for some successive faucet openings.

III. RESULTS AND DISCUSSION

Crisis

An overview from 9.8 drops/s up to 39.7 drops/s is shown in Fig. 3, where we sequentially plotted t_n vs n as

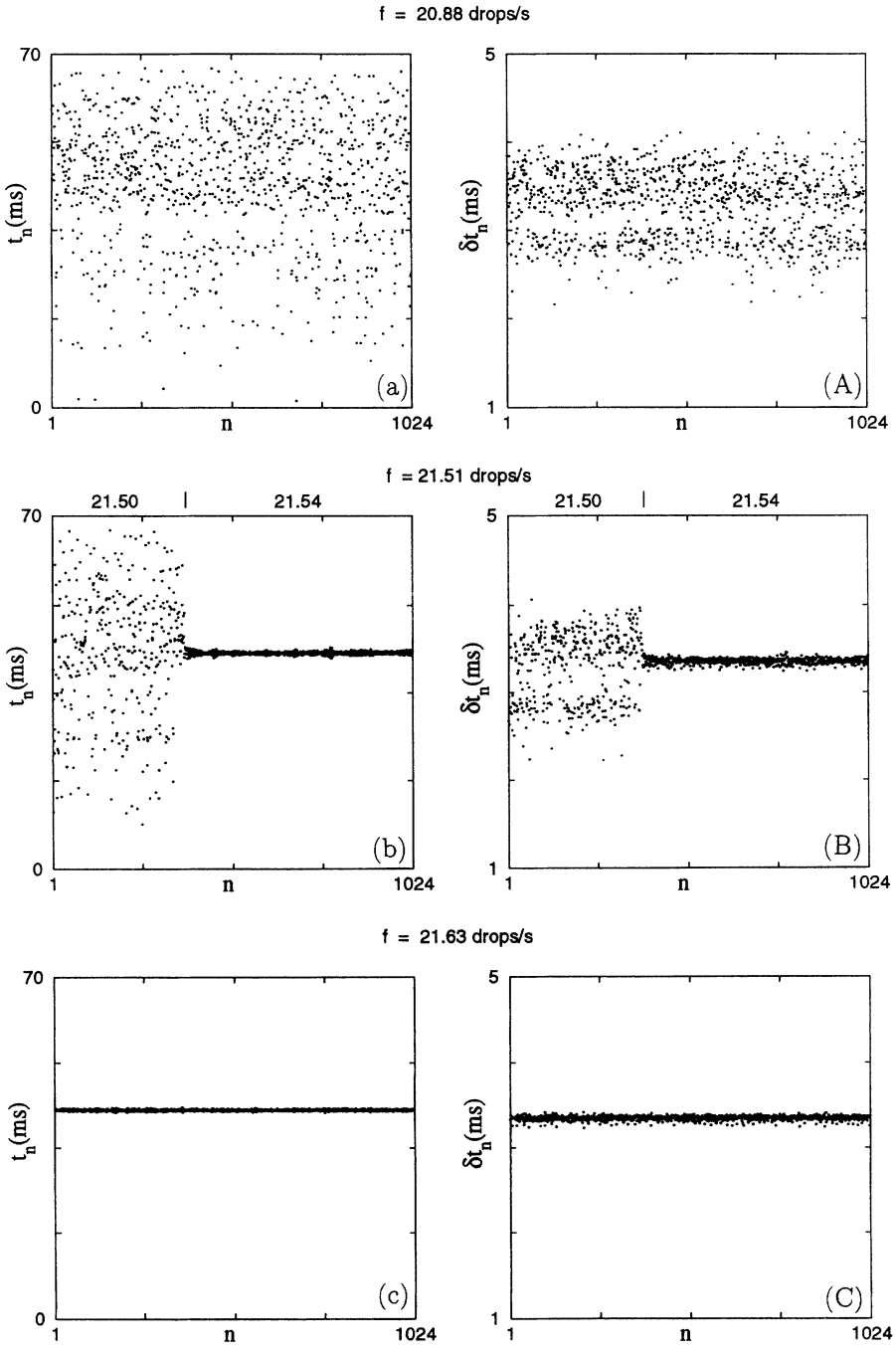

FIG. 5. Plots of t_n vs n (left) and δt_n vs n of the same sequence shown in Fig. 4. In (b) and (B) we show the transition from chaotic to period-1 behavior.

well as δt_n vs n, of a sequence of 208 sample data (each sample corresponds to 1024 drops).

The graph of δt_n vs n shows 4 plateaus of $\delta t_{n_{max}} =$ 5.1, 4.1, 3.9, and 3.0 ms, respectively. The circles are a crude estimation of the maximum drop size, as obtained in another run, when we recorded the drop motion together with a graduated scale illuminated by a stroboscopic light. For a given water flux we selected some drops and among these we chose the ones with the biggest diameter. For each $\delta t_{n_{max}}$ plateau we have $D_{max} \simeq 7$, 7, 6, and 5 mm, respectively. The values of δt_{nmax} are probably given by those drops that have zero escape speed. Supposing that they are the biggest ones, their speeds $v = D_{max}/\delta t_{n_{max}}$ at the laser beam level are 137, 171, 154, and 167 cm/s, respectively. Taking into account the crudity of these calculations, we can say that these speed values are in agreement with the speed given by

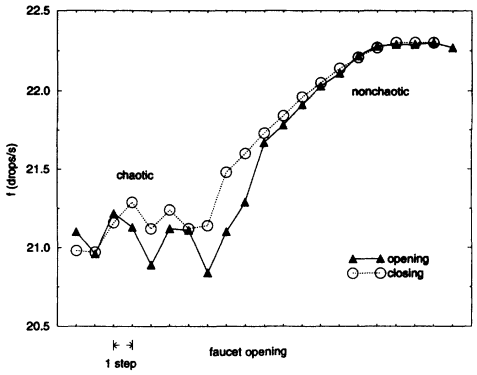

FIG. 6. The mean drop frequency as a function of the faucet opening around the I transition. Every point is the average of four cycles.

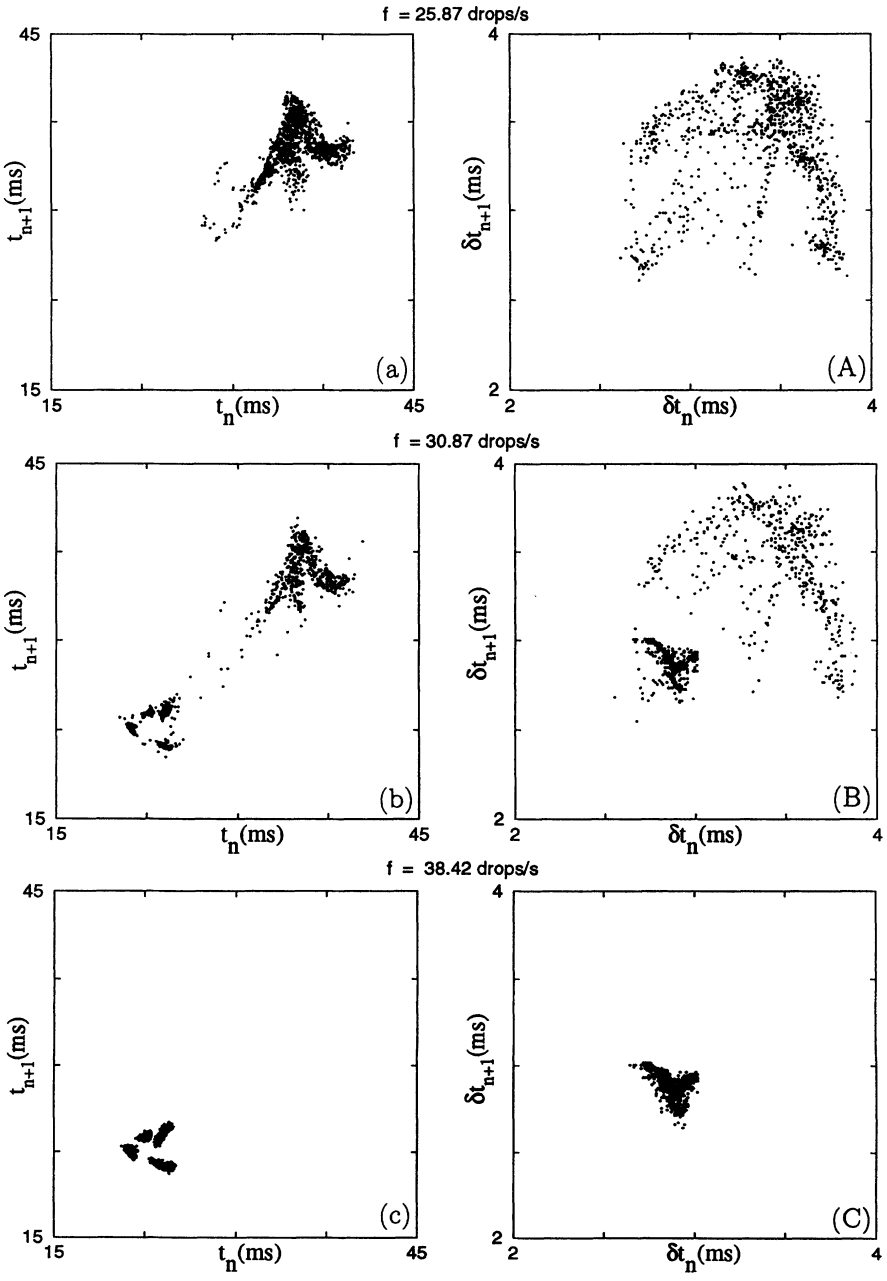

FIG. 7. Return maps t_{n+1} vs t_n (left) and δt_{n+1} vs δt_n (right). In (b) and (B) we show the transition from chaotic to period-5 behavior.

$v = \sqrt{2gh} \approx 128$ cm/s, where $h \approx 8.4$ cm is the distance between the laser beam level and the drop breakaway position.

The sudden changes from chaotic to periodic regimes, labels I and B shown in Fig. 3, detected by the two types of variables (t and δt), were investigated, as we will see below. A sequence of three data samples around the I transition is shown in Fig. 4. At the left we have the return maps t_{n+1} vs t_n and, at the right we have the return maps δt_{n+1} vs δt_n. In Fig. 5 we have the same sequence in the t_n vs n (δt_n vs n) plotting form.

The sample data in Figs. 4(a) and 4(A) [or in Figs. 5(a) and 5(A)] shows a chaotic behavior with a mean drop frequency of $f = 20.88$ drops/s. In Figs. 4(b) and 4(B) the system started in a similar chaotic regime as before and suddenly changed to a period-1 regime. A better view of this transition is shown in Figs. 5(b) and 5(B); despite this drastic change in the attractors, the mean drop frequency changed a little, from $f = 21.50$ drops/s in the chaotic regime to $f = 21.54$ drops/s in the period-1 regime. The final period-1 regime ($f = 21.63$ drops/s) is confirmed in Figs. 4(c), 4(C), 5(c), and 5(C).

After that, to investigate if this transition was not due to a random disturbance, we collected an opening faucet

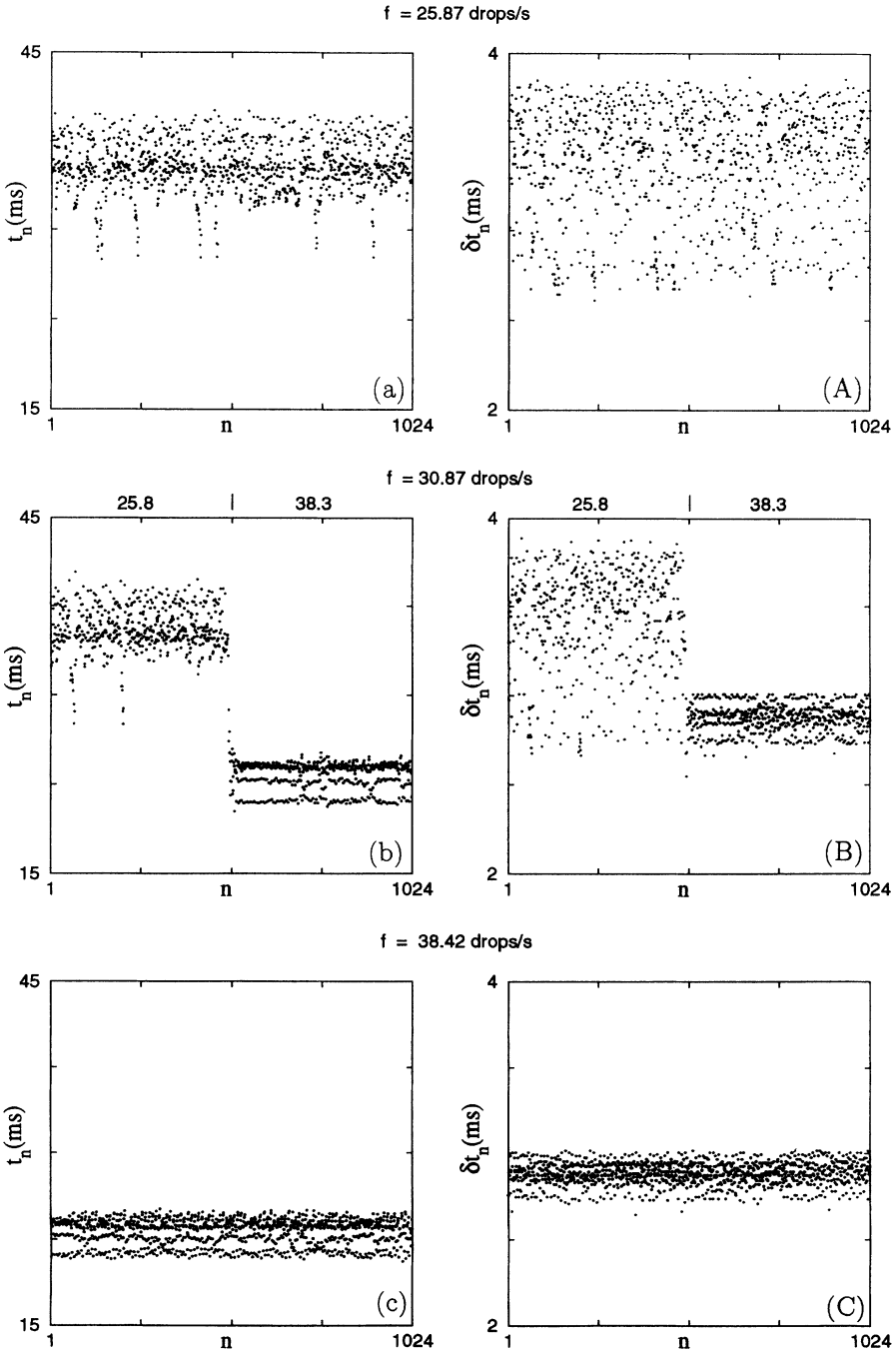

FIG. 8. Plots of t_n vs n (left) and δt_n vs n (right) of the same sequence shown in Fig. 7. In (b) and (B) we show the transition from chaotic to periodic behavior.

sequence, followed by a closing sequence, around $f \simeq 21.5$ drops/s, each sequence with 20 data samples. This cycle was repeated four times. In Fig. 6 we have the mean drop frequency as a function of the faucet opening, where the triangle signs are the data of the opening run and the circles are the data closing the faucet. Each point corresponds to the averaged value of the four runs in the same faucet opening. Below the ninth step we have chaotic attractors and, above, nonchaotic attractors. No appreciable hysteresis was observed.

Data around the B transition are shown in Fig. 7 (t_{n+1} vs t_n and δt_{n+1} vs δt_n return maps) and Fig. 8 (t_n vs n and δt_n vs n plotting form).

In Figs. 7(a) and 7(A) [or in Figs. 8(a) and 8(A)] we have a chaotic state with a mean drop frequency $f = 25.87$ drops/s. In Figs. 7(b) and 7(B) the system started in a similar chaotic state as before and suddenly changed to another state. In this case occurred a drastic change in the mean drop frequency, from $f \simeq 25.8$ drops/s in the chaotic state to $f \simeq 38.3$ drops/s in the final state, as shown in Figs. 8(b) and 8(B). The two drop frequencies, $f \simeq 25.87$ drops/s and $f \simeq 38.3$ drops/s, defined a region of forbidden attractors, that is, we could not get any attractor with a mean drop frequency with an intermediate value between these two frequencies.

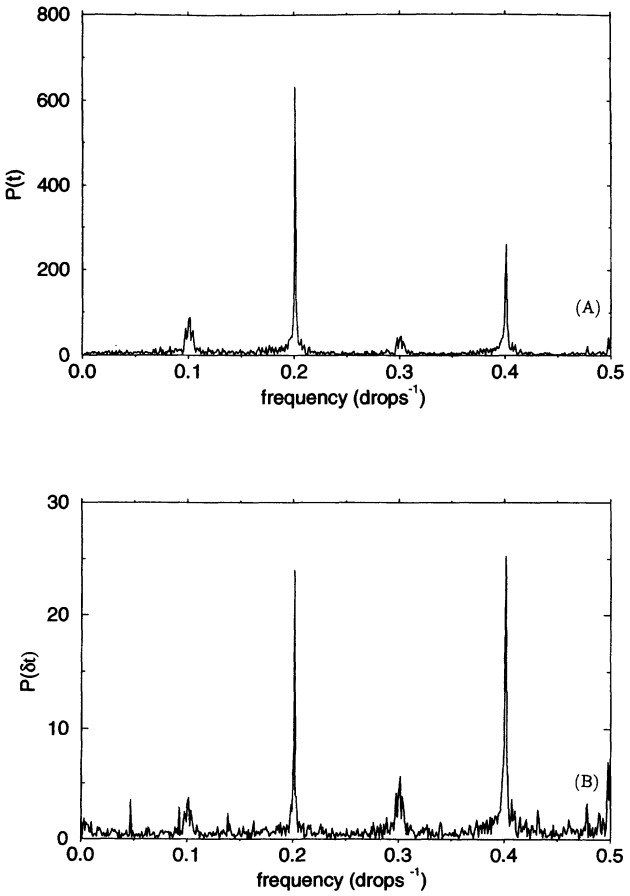

FIG. 9. Fast Fourier transform power spectra $P(t)$ and $P(\delta t)$ of the data shown in Figs. 8(c) and 8(C).

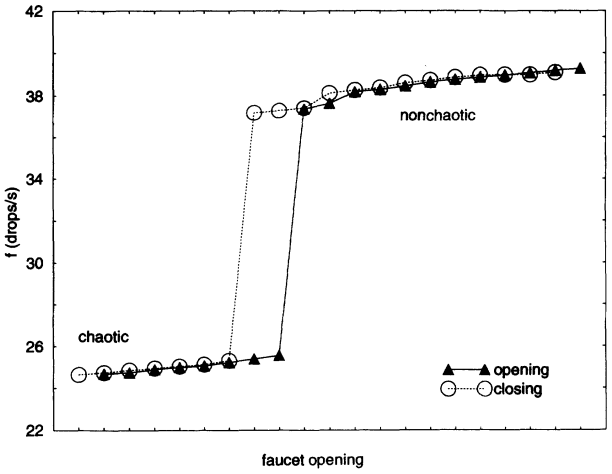

FIG. 10. The mean drop frequency as function of the faucet opening around the B transition. Every point is the average of 4 cycles. An hysteresis of two steps is observed.

To determine the periodicity of the final state above, we calculated the FFT power spectra of $t(n) - \langle t \rangle$ and $\delta t(n) - \langle \delta t \rangle$ using the data shown in Figs. 8(c) and 8(C). The results $P(t)$ and $P(\delta t)$ are shown in Figs. 9(A) and 9(B), respectively. These spectra show five commensurate frequencies, 0.1, 0.2, 0.3, 0.4, and 0.5 drops^{-1}, with the highest intensities corresponding to the frequencies of 0.2 and 0.4 drops^{-1}. Therefore the periodicity is of five drops.

As before, we did measurements around the transition, opening (closing) the faucet in four cycles. In Fig. 10 we have the mean drop frequency as a function of the faucet opening, where the triangle signs are the data average of the four runs opening the faucet and the circles

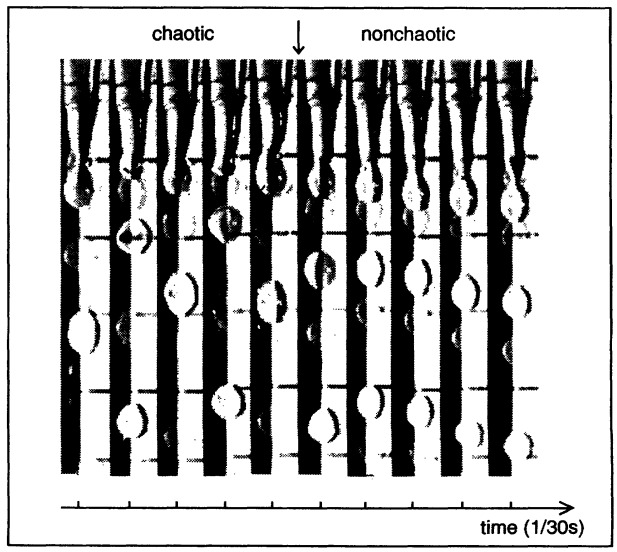

FIG. 11. Recorded drop motion, at 30 frames per second, showing the transition from chaotic (the first five frames) to a period-5 behavior (the last five frames).

correspond to the averaged data closing the faucet. A hysteresis of two steps was observed.

In Fig. 11 we have the digitized images of the motion, for ten successive video frames, showing the transition from chaotic to the period-5 behavior. In the chaotic regime there is a vibration motion of the water column, with the water cone vertex unstable, with a different break away position for each drop. After changing to the nonchaotic regime, the water column vibration seems to cease, with the water cone vertex stable, giving the same break away position for all drops.

Therefore, it seems that the system destroyed the basin

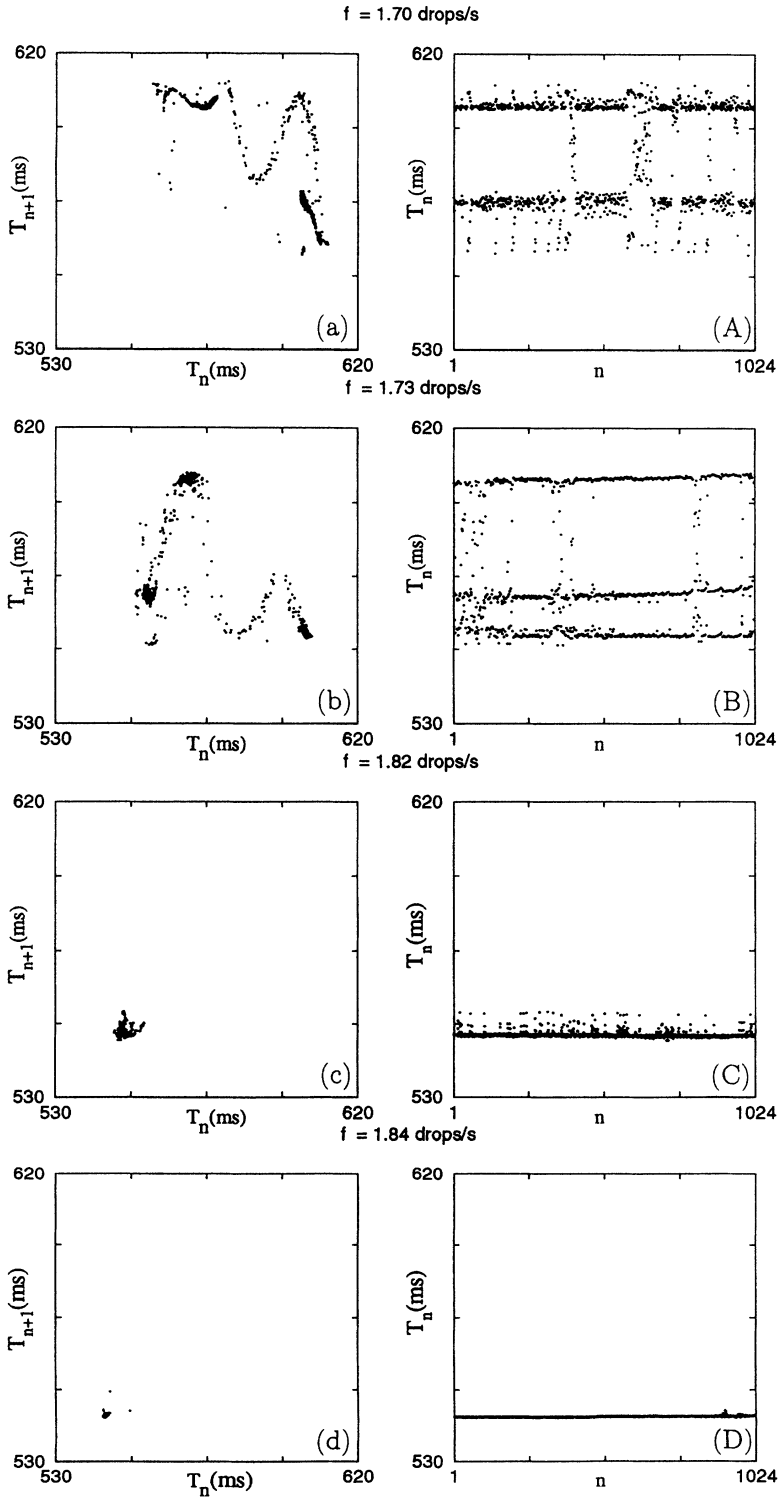

FIG. 12. A sequence that shows a tangent intermittence between chaos and period-3 attractors for low drop frequency ($f \simeq 1.7$ drops/s).

of a chaotic (nonchaotic) attractor and created the basin of a nonchaotic (chaotic) attractor as in the case of the boundary crisis described by Grebogi *et al.* [6].

IV. INTERMITTENCIES

Intermittence between chaos and period-3 attractors, associated with a tangent bifurcation as explained by Manneville and Pomeau [7], were observed for low drop frequency ($f \simeq 1.7$ drops/s) and for $f \simeq 15.3$ drops/s.

The sequence shown in Fig. 12 corresponds to the low frequency data, where the graphs at the left are the T_{n+1} vs T_n plots and the ones at the right the T_n vs n plots. In Figs. 12(A) and 12 (B) we show a periodic behavior with bursts of chaos.

The sequence of data for the higher drop frequency is shown in Fig. 13 (see the periodic window $I3$ in Fig. 3), where the graphs at the left are the t_{n+1} vs t_n return maps and the ones at the right the δt_{n+1} vs δt_n return maps. In Fig. 14 we show the same sequence in the t_n vs n (δt_n vs n) plotting form. A periodic behavior

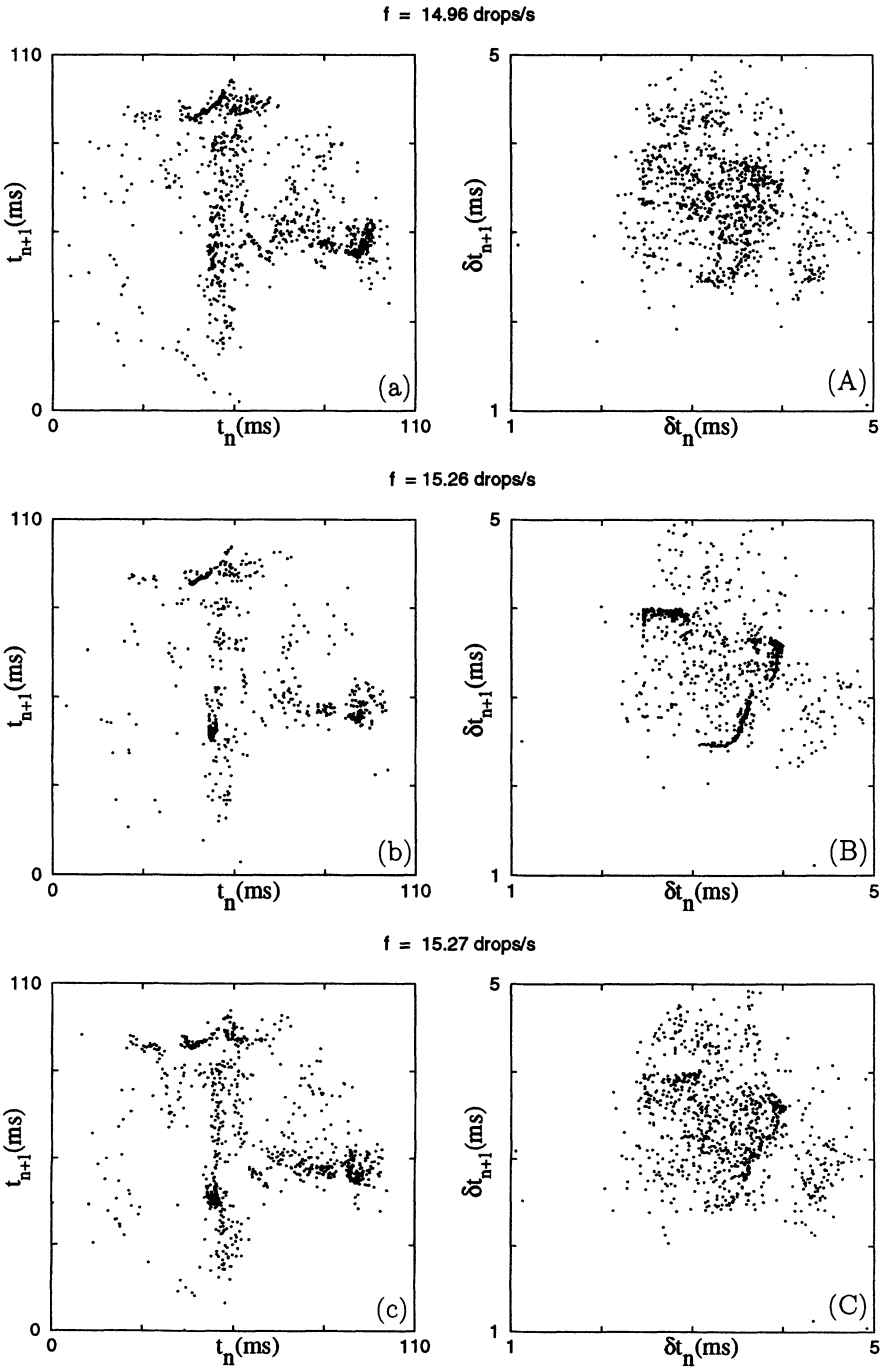

FIG. 13. Return maps t_{n+1} vs t_n (left) and δt_{n+1} vs δt_n (right), around $f \simeq 15.2$ drops/s.

with bursts of chaos is also shown in the Fig. 14(b), and 14(B). The behaviors shown in Figs. 12(A), 12(B), 14(b), and 14(B) are similar to the behaviors obtained from a one-dimensional map, $t_{n+1} = pt_n(1 - t_n)$, for $p \lesssim 3.82\cdots = p_3$. As in this case there is a tangent bifurcation, we should have a tangent intermittence.

A new intermittent behavior between even periodic attractors was observed for low drop frequency, $f \simeq 1$–3 drops/s. In Fig. 15 we show a sequence of data, where the graphs at the left are the T_{n+1} vs T_n return maps and the ones at the right are the T_n vs n plots.

In Figs. 15(a) and 15(A) we show a period-1 attractor, and in Figs. 15(b) and 15(B) we show a period-2 attractor. In Fig. 15(c) we show a presumably period-2 attractor, but in Fig. 15(C) we can observe that is an intermittent regime between period-2 and a period-4 attractors. In Figs. 15(d) and 15(D) the system returned to a period-1 attractor.

In Fig. 16, we have a similar sequence as before for a slightly higher water flux ($f \simeq 1.6$ drops/s). A period-2 attractor, Figs. 16(b) and 16(B), followed by an intermittent behavior between period-2 and period-4 attractors,

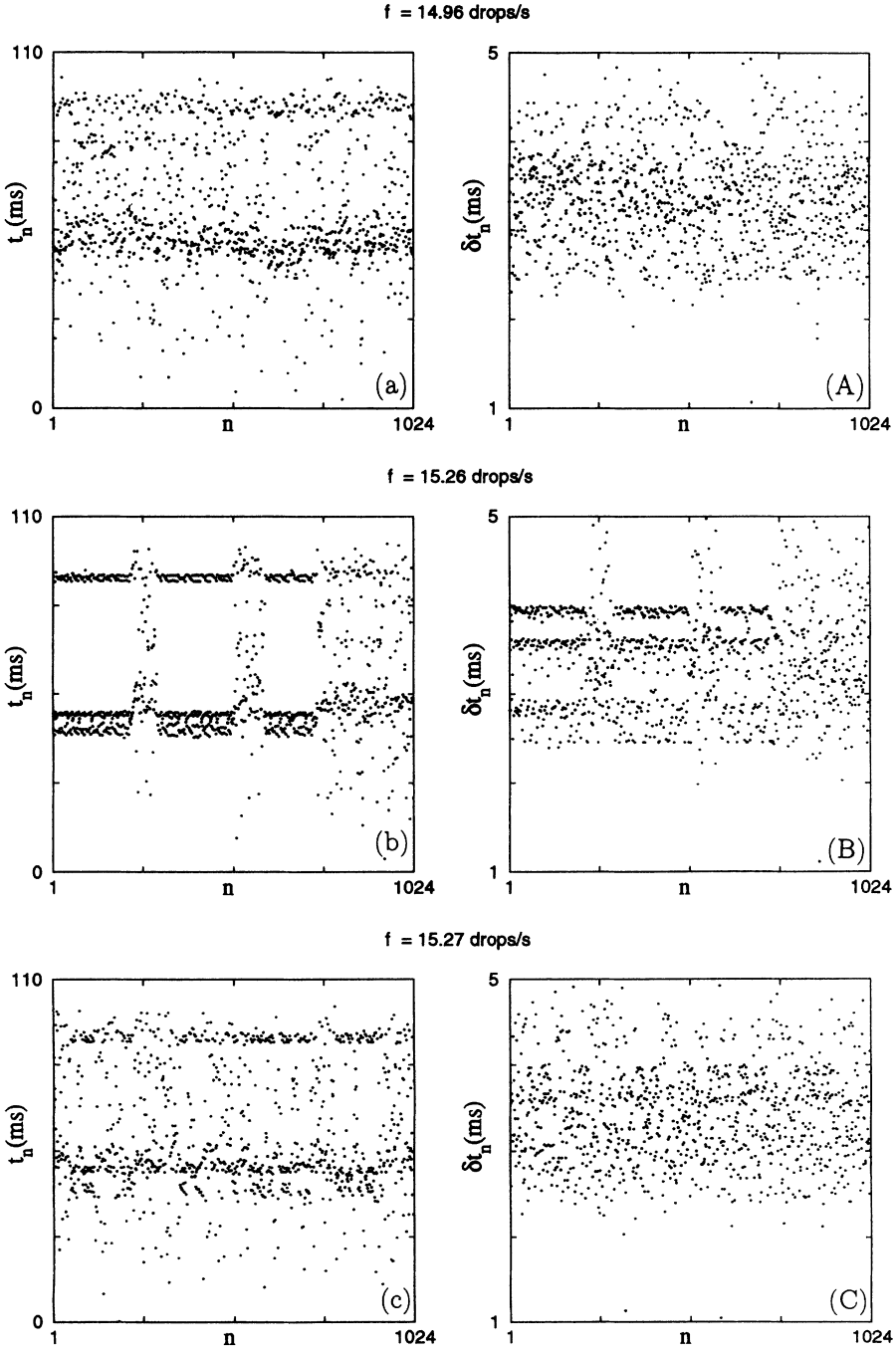

FIG. 14. The same sequence of data of Fig. 12, t_n vs n (left) and δt_n vs n (right), showing a tangent intermittence between chaos and period-3 attractors.

Figs. 16(c) and 16(C), followed by a period-1 attractor, Figs. 16(d) and 16(D).

The very small instabilities in the period-1 attractors and intermittencies between even periodic attractors were observed only for low mean drop frequency or long time drop formation. This intermittence could be attributed to the noise in some parameter of the equation of motion, originated by small temperature fluctuations or by the vibrations of very small air bubbles in the water circuit. But the data shown in Figs. 15 and 16 for two different drop frequencies respectively follow the same sequence of attractors:

$$\text{period-2} \rightarrow \text{intermittence } 2 \Longleftrightarrow 4 \rightarrow \text{period-1}.$$

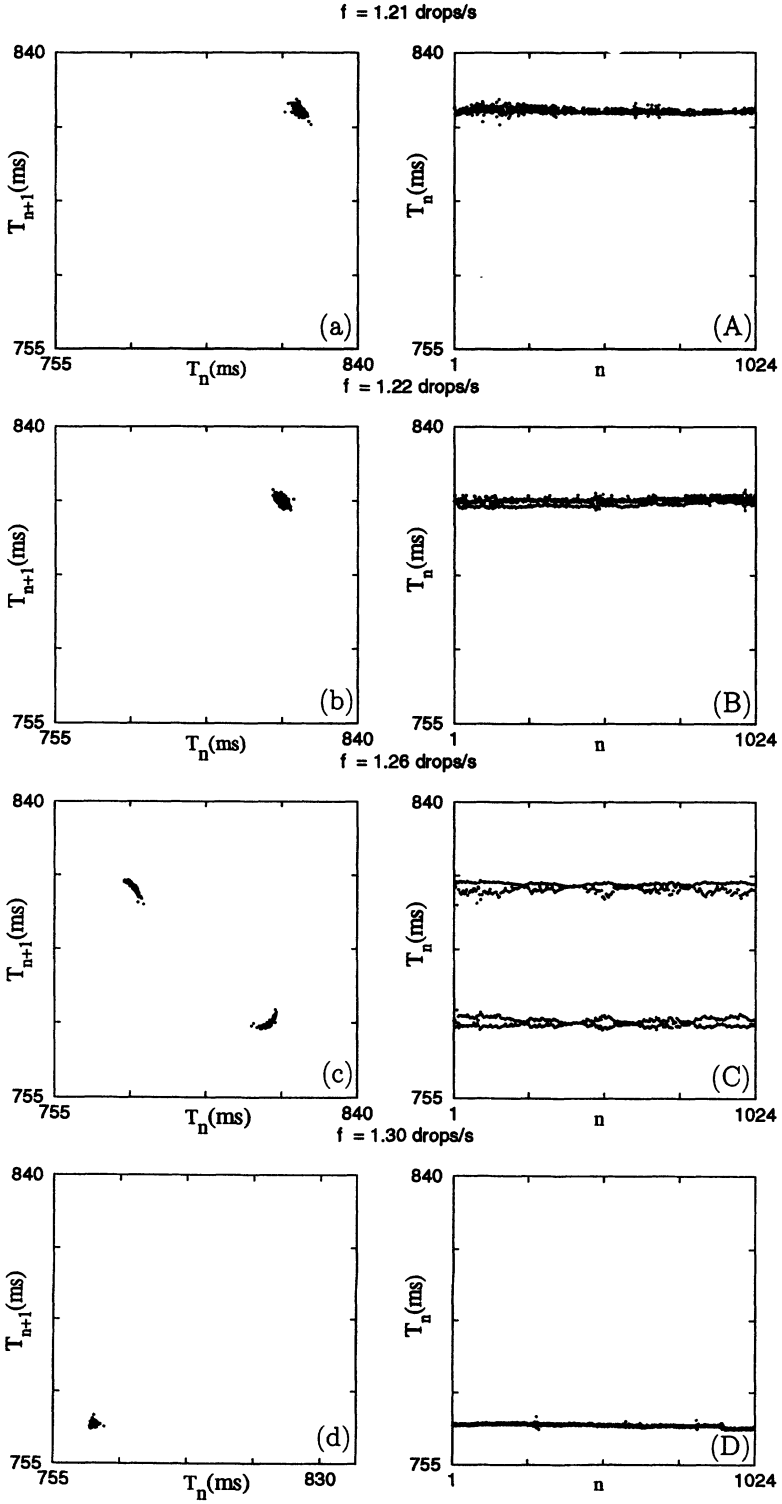

FIG. 15. Return map T_{n+1} vs T_n (left) and T_n vs n (right) around $f \simeq 1.26$ drops/s. This sequence shows intermittence between even periodic attractors.

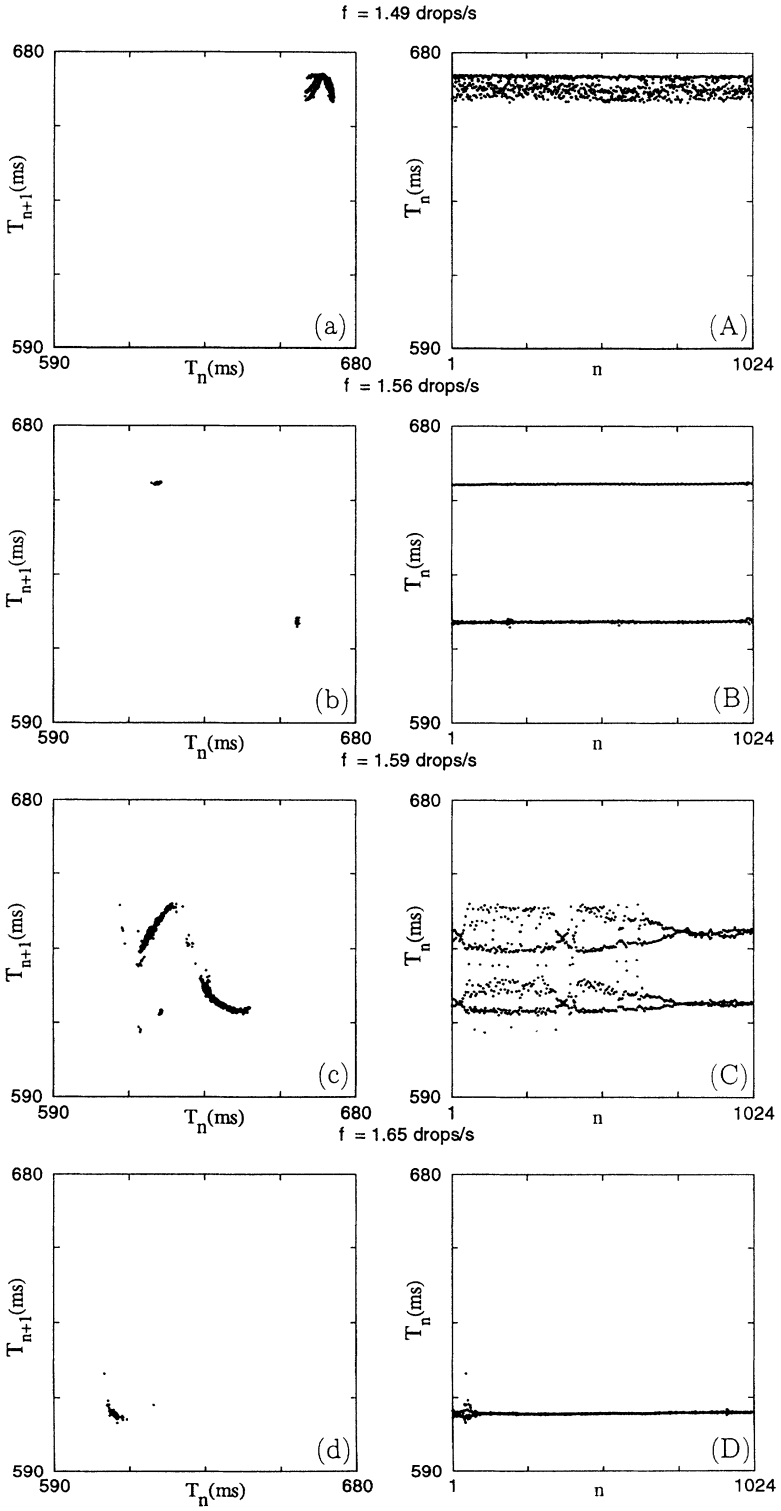

FIG. 16. A similar sequence as in Fig. 15, showing intermittence between even periodic attractors, around $f \simeq 1.6$ drops/s.

Therefore this kind of intermittent pattern can be a characteristic of the dynamical system. Data concerning quasiperiodic motions and other data will be reported later.

V. CONCLUSION

The stability shown by the water system, together with the good resolution and accuracy to measure the time between drops, allowed the observation of two types of sudden changes in chaotic attractors, one of them consistent with a boundary crisis interpretation.

Furthermore, intermittencies of two types were observed. One of them is associated with tangent bifurcation with odd periodic attractors and bursts of chaos. The other one is an intermittent behavior between two even periodic attractors (period-2 and period-4) hidden inside a presumably period-2 attractor.

[1] P. Martien, S. C. Pope, P. L. Scott, and R. S. Shaw, Phys. Lett. **110A**, 339 (1985).
[2] H. N. N. Yépez, A. L. S. Brito, C. A. Vargas, and L. A. Vicente, Eur. J. Phys. **10**, 99 (1989).
[3] R. F. Cahalan, H. Leidecher, and G. D. Cahalan, Comp. Phys. **4**, 368 (1990).
[4] X. Wu and Z. A. Schelly, Physica D **40**, 433 (1989).
[5] K. Dreyer and F. R. Hickey, Am. J. Phys. **59**, 619 (1991).
[6] C. Grebogi, E. Ott, and J. A. Yorke, Physica D **7**, 181 (1983); Phys. Rev. Lett. **48**, 1507 (1982).
[7] P. Manneville and Y. Pomeau, Physica D **1**, 219 (1980).

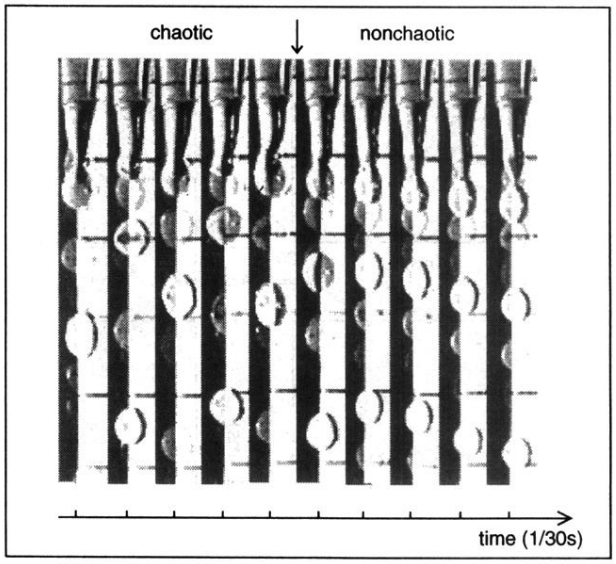

FIG. 11. Recorded drop motion, at 30 frames per second, showing the transition from chaotic (the first five frames) to a period-5 behavior (the last five frames).

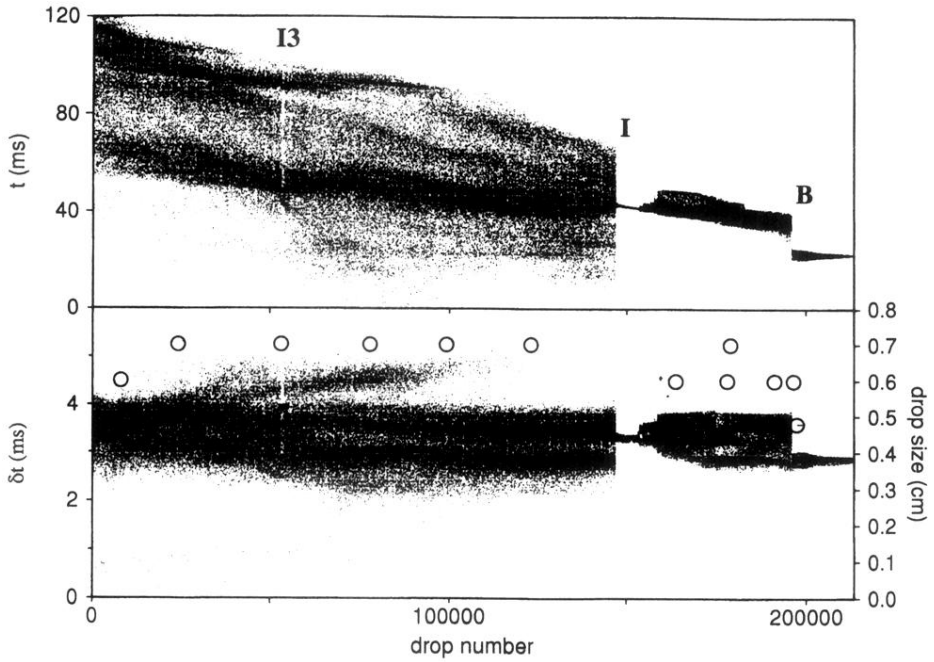

FIG. 3. An overview of a sequence of 208 sample data (each sample has 1024 data); t_n is the time between drops and δt_n is the crossing time through the laser beam. The discontinuity B is consistent with a boundary crisis interpretation. $I3$ is a periodic window. The circles are a crude estimation of the drop size.